

## **EFFECT OF AGGREGATE ON FRACTURE PROPERTIES OF HIGH-PERFORMANCE CONCRETE**

T.P. Chang, K.L. Tsao and B.R. Lin

Department of Construction Engineering, National Taiwan University of Science and Technology, Taiwan, R.O.C.

B.R. Lin

Department of Civil Engineering, Tung Nan Junior College of Technology, Taiwan, R.O.C.

### **Abstract**

The fracture properties of the high-performance concrete (HPC) having a slump of 260 mm, flowability of 680 mm, 28-day compressive strength of 64.7 MPa and modulus of elasticity of 25.1 GPa were studied. The size-effect law was used for examining the fracture properties. Experimental results show that the size of coarse aggregate and the amount of aggregate in the HPC have positive effects on the increase of its fracture properties. The value of fracture energy  $G_y$  of the HPC was found to be 68.3 N/m. When same volumetric amount of coarse aggregate in the HPC was replaced by the fine aggregate, the fracture energy  $G_y$  was dropped to the value of 22.5 N/m. The fracture energies of the hardened binder paste and cement paste range from 3.4 to 3.5 N/m.

**Key words:** Aggregate, fracture property, high-performance concrete.

## 1 Introduction

In addition to three major conventional ingredients used in the normal concrete, i.e., the Portland cement, fine and coarse aggregates and water, the making of high-performance concrete (HPC) needs to incorporate the supplementary mineral admixture such as silica fume, fly ash and blast-furnace slag, etc., and chemical admixture such as superplasticizer, etc., in order to have a high workability without segregation and high strength [Okamura 1997, Aitcin et al. 1993, Gutiérrez et al. 1996, Mehta et al. 1990]. There is no unique definition of HPC. The essence of HPC is emphasized on the performance requirement of the intended use of the concrete. In general, an HPC with an initial slump of more than 250 mm and a 28-day compressive strength of above 55 MPa can be regarded as the concrete having a high workability and high strength. Since the increasing demanding of applying the HPC to the various kinds of concrete constructions, the understanding of its fracture properties is useful for the designer to use the fracture criteria for the prediction of catastrophic crack propagation of the concrete structure under certain loading conditions. The purpose of this study is aiming at the effects of aggregate on the fracture properties of high-performance concrete based on the well-known size-effect model.

## 2. Calculation of fracture energy based on size-effect model

Three test methods have been recommended by the RILEM Technical Committee 50-FMC and TC89-FMT for measuring the fracture energy of concrete based on different fracture mechanics concepts, i.e., the fictitious crack model [Hillerborg et al. 1976], the two-parameter fracture model [Jenq and Shah, 1985], and the size-effect model [Bazant et al. 1987], respectively. The size-effect model was used in this study. According to this model, the geometry of the single-edge-notched three-point-bend (SEN-TPB) beam specimen used in this study is shown in Fig. 1. At least three sizes of specimens with a scale ratio of at least 4 must be used. Then the fracture energy  $G_f$  of the concrete can be calculated by the following equation [Bazant et al. 1987]:

$$G_f = \frac{B^2 (f_u)^2}{c_n^2 E'} d_0 g(\alpha_0) \quad (1)$$

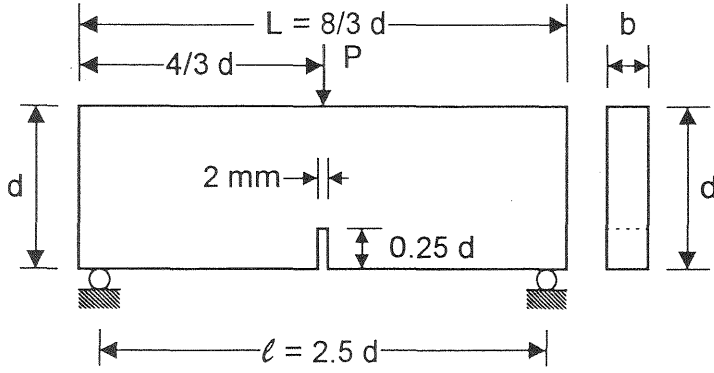


Fig. 1. Single-edge-notched three-point-bend (SEN-TPB) beam specimen

where  $E' = E$  for plane stress and  $E' = E/(1-\nu^2)$  for plane strain;  $E$  = modulus of elasticity;  $\nu$  = Poisson's ratio;  $f_u$  = tensile strength of concrete;  $c_n = 1.5\ell/[d(1-\alpha_0)^2]$ ;  $\ell$ ,  $d$  = span and height of the specimen, respectively;  $\alpha_0 = a_0/d=0.25$ ;  $a_0$  = initial depth of the notch;  $g(\alpha)$  is the geometric factor of the specimen and, for this case of  $\ell/d = 2.5$ , is given as

$$g(\alpha) = \left[ \frac{6.647\sqrt{\alpha} \left( 1 - 2.5\alpha + 4.49\alpha^2 - 3.98\alpha^3 + 1.33\alpha^4 \right)}{(1-\alpha)^{1.5}} \right]^2 \quad (2)$$

Based on the size-effect law, the values of two constant  $B$  and  $d_0$  in Eq. (1) can be determined from the test data of SEN-TPB beam directly through the following nonlinear regression:

$$\sigma_N = B \frac{f_u}{(1 + d/d_0)^{0.5}} \quad (3)$$

in which  $\sigma_N = P_{\max}/(bd)$ ;  $P_{\max}$  = maximum failure load;  $b$  = thickness of the specimen. Or these two values can be simply calculated from the following linear regression:

$$Y = AX + C \quad (4)$$

$$X = d; Y = \left( \frac{f_u}{\sigma_N} \right)^2; \sigma_N = c_n \frac{P_{\max}}{bd}; B = \frac{1}{\sqrt{C}}; d_0 = \frac{C}{A} \quad (5)$$

In general, the values of B and  $d_0$  obtained from Eqs. (3) and (4) are different, but both sets can be legitimately used in the calculation of fracture energy. The linear regression approach was used in this study.

### 3. Materials

Portland Type I cement meeting the requirements of ASTM C150 was used for all the experiments. The coarse aggregate obtained from the crushed sandstone had its percents retained on the sieves of 4.7% (12.7 mm), 38% (9.5 mm) and 57.3% (4.75 mm), which led to a fineness modulus of 6.47. The specific gravity and absorption for coarse aggregate were 2.65 and 0.91%, respectively. The fine aggregate was a natural river sand, having a specific of 2.65, an absorption of 2.1 percent, and a fineness modulus of 2.89. A type F fly ash having a specific gravity of 2.21, a blast-furnace slag having a specific gravity of 2.87, and an ASTM Type G liquid superplasticizer were used in the test.

### 4. Experimental program

Four different types of specimen mixtures were used, i.e., the normal high-performance concrete (HPC), fine-aggregate concrete (HPCs), binder paste (HPCb), and cement paste (HPCp). The fine-aggregate concrete (HPCs) was obtained by replacing all the coarse aggregate in the mixture of normal high-performance concrete (HPC) with a same volumetric amount of the fine aggregate. The binder paste was made purely by the paste in the HPC, which only contained water, cement, fly ash, blast-furnace slag and superplasticizer. Finally, the cement paste (HPCp) was composed of only same proportion of those water and cement that were used in casting the high-performance concrete (HPC). The proportioning of the four mixtures is summarized in Table 1.

Cylinders of  $\phi 100 \times 200$  mm for compressive tests, splitting tensile test and test for modulus of elasticity were cast and tested using a 200 kN compression machine according to ASTM C469 and ASTM C496,

respectively. Four different sizes of SEN-TPB beam specimens ( $40 \times 40 \times 110$ ,  $40 \times 80 \times 210$ ,  $40 \times 160 \times 430$ ,  $40 \times 320 \times 850$  mm) with a notch width of 2 mm for the fracture energy test were cast and tested using a 100 kN MTS machine with a close-loop-controlled stroke system. There were three specimens tested for each set of experiment. All the specimens were stored in the saturated lime water under a temperature of  $23 \pm 2$  °C until one day before the test.

Table 1. Proportion of the concrete mixture ( $\text{kg/m}^3$ )

Item	Normal HPC	Fine aggregate HPCs	Binder HPCb	Cement HPCp
Coarse aggregate	1018	0	0	0
Fine aggregate	708	1726	0	0
Cement	382	382	1096	1342
fly ash + slag	145	145	416	0
Superplasticizer	21	21	15	3
Water	163	163	469	574
W/C	0.43	0.43	0.43	0.43

## 5. Test results and discussion

The compressive strength  $f_c$ , splitting tensile strength  $f_u$ , modulus of elasticity  $E_c$ , Poisson's ratio  $\nu$ , slump, and flowability for four kinds of specimen mixtures tested in this study are shown in Table 2.

Table 2. Engineering properties of specimens

Item	HPC		HPCs		HPCb		HPCp	
	28	56	28	56	28	56	28	56
age (day)	28	56	28	56	28	56	28	56
$f_c$ (MPa)	64.7	67.2	40.7	50.7	71.0	75.2	52.7	54.4
$f_u$ (MPa)	—	4.18	—	3.58	—	3.20	—	1.39
$E_c$ (GPa)	25.1	26.3	21.0	22.9	18.7	19.8	12.6	15.2
$\nu$	0.12	0.10	0.15	0.12	0.20	0.18	0.15	0.18
Slump (mm)	260		10		> 280		> 280	
Flowability (mm)	660		200		> 700		> 700	

Note: — data unavailable

With a careful and logical rule to make the concrete proportioning, the slump and flowability of the high-performance concrete (HPC) was found to be 260 mm and 660 mm, respectively. The compressive strength  $f_c$  and modulus of elasticity  $E_c$  at age of 28 days were 64.7 MPa and 25.1 GPa. Because of the increase of larger surface area of the replacing fine aggregate, the slump and flowability of fine-aggregate concrete HPCs reduced abruptly. The hardened binder paste has the highest compressive strength among four specimen mixtures, which indicates, in addition to the durability consideration, the positive gain of material strength by adding the mineral admixture in the mixture of high-performance concrete. Due to a better packing structure for the aggregate mixture of coarse and fine particles in the concrete, the compressive strength of high-performance concrete (HPC) is higher than that of the fine-aggregate concrete (HPCs).

The test data from the fracture experiments for all the SEN-TPB beam specimens are shown in Table 3. Typical point load-CMOD (Crack-mouth-opening-displacement) curves for the high-performance concrete HPC and the cement paste HPCp at the age of 56 days are shown in Fig. 2(a) and (b).

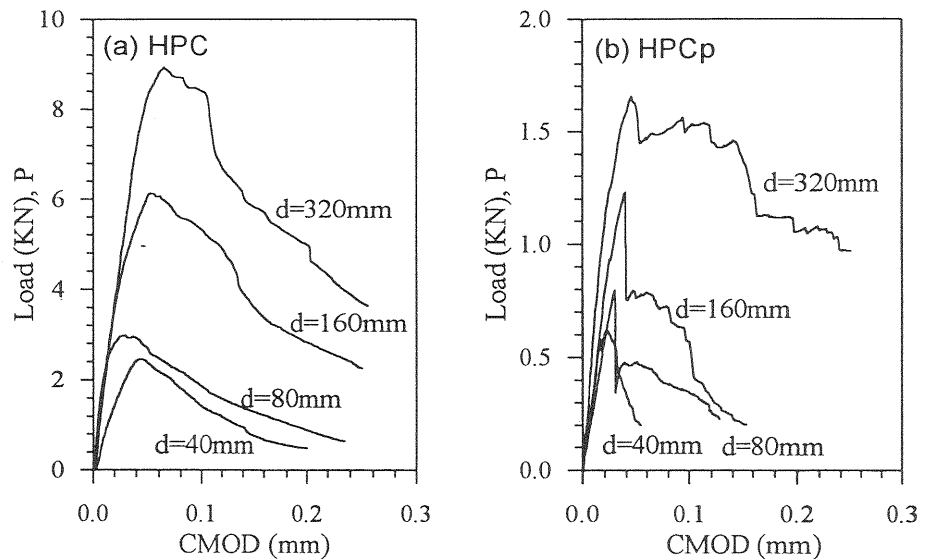


Fig. 2. Typical load-CMOD (crack-mouth-opening-displacement) curves for four different sizes of SEN-TPB beam specimen cast by (a) high-performance concrete (HPC) and (b) cement paste (HPCp)

Table 3 Maximum center loads  $P_{max}$  on four SEN-TPB specimens

Type	age (day)	d (mm)	$P_{max}$ (N)			A ( $m^{-1}$ )	C	B	$d_0$ (mm)	$G_f$ (N/m)
			# 1	#2	#3					
HPC	56	40	1802	2389	2467	2.06	0.141	2.667	68.30	68.3
		80	2990	3714	—					
		160	5781	6852	6147					
		320	9025	8708	8892					
HPCs	56	40	1762	1925	2406	5.25	0.014	8.439	2.674	22.5
		80	2738	3248	—					
		160	3425	3525	—					
		320	4708	5632	5891					
HPCb	56	40	528	746	700	31.3	0.254	4.683	8.126	3.48
		80	—	1142	—					
		160	1655	1060	1296					
		320	1980	1911	—					
HPCp	56	40	694	606	592	6.75	0.046	4.683	6.756	3.40
		80	835	795	—					
		160	1228	1355	—					
		320	1654	1980	—					

Notes: —: unavailable due to bad specimen condition.

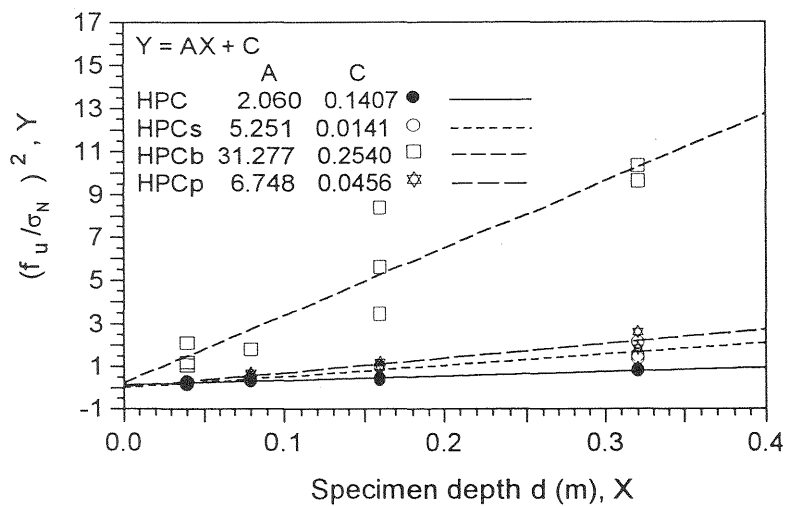


Fig. 3. Linear regression lines and values of constants

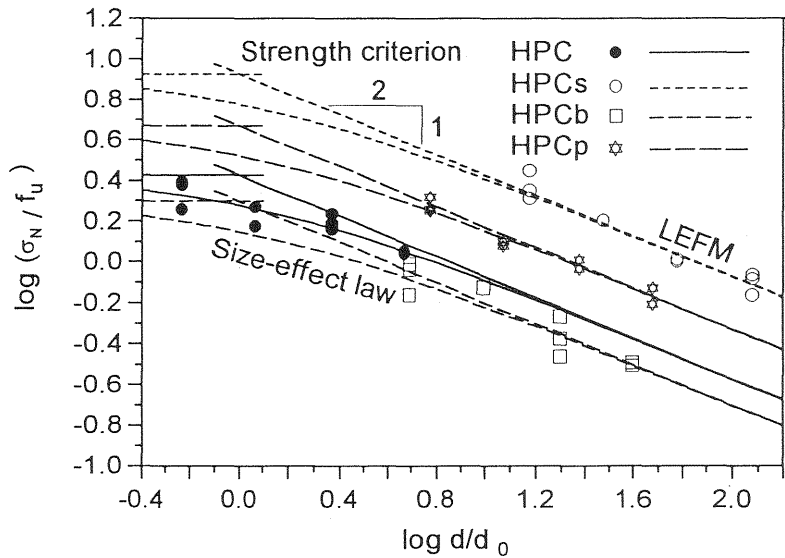


Fig. 4. Size-effect curves for four SEN-TPB beam specimens

Since the considerably brittle properties of the hardened cement paste (HPCp), the response after the peak load exhibits an unstable and abrupt up-and-down manner as shown in Fig. 2(b). Similar pattern was also found in the hardened binder paste (HPCb). By using Eqs. (4) and (5), the linear regression lines and the values of constants  $A$  and  $C$  for all the test data are shown in Fig. 3. Because of a relatively higher tensile strength of the hardened binder paste (HPCb), the slope of its linear regression line is much steeper than those of the other three mixtures as shown in Fig. 3. By using Eqs. (1), (2), (4) and (5), the fracture energies  $G_f$  for four mixtures are obtained and shown Table 3. The resulting size-effect curves based on these given values are illustrated in Fig. 4.

Although it has been well-known that the hardened concrete usually has a higher fracture energy than the hardened mortar and cement paste, it is quite surprised to note that, from the test results in this study, there is a tremendously higher fracture energy of 68.3 N/m for high-performance concrete (HPC), as comparing with those values of 22.5 N/m (HPCs), 3.48 N/m (HPCb) and 3.40 N/m (HPCp). For normal strength concrete, the value of  $G_f$  was about 24.1 N/m for  $f_c = 36.9$  MPa at age of 28 days ( $G_f \cong 21.4$  N/m for  $f_c = 32.5$  MPa at age of 14 days), and 85.5 MPa N/m for high-strength concrete ( $f_c = 85.5$  MPa at age of 14 days) [Gettu et al. 1990]. But the values of  $G_f$  seem to be rather scatter. Other paper reported that

$G_f = 14.6$  N/m for normal concrete with  $f_c = 21$  MPa, and  $G_f = 45.1$  N/m for high-strength concrete with  $f_c = 62.6$  MPa [Perdikaris et al. 1995]. In current study, the pozzolanic reaction between the mineral admixture and calcium hydroxide in the product of cement hydration helps increase the strength of cement paste and interface strength on the aggregate surface of high-performance concrete. This is part of the reason that high-performance concrete has a better fracture energy. The test data confirms that the inclusion of a certain amount and size of coarse aggregate in the HPC is necessary and beneficial to both the concrete strength and fracture energy. On the other hand, the hardened binder paste (HPCb) has the highest compressive strength, but its fracture energy is also almost the lowest. Maintaining same volumetric amount of coarse aggregates but with the smaller size in the high-performance concrete (HPCs) will reduce the fracture energy substantially. The correlation between the strength and fracture energy varies considerably and randomly in the current study. This observation indicates that the strength of concrete seems not the only criterion to infer the value of its corresponding fracture energy. Other factors such as the characteristics of packing structure of aggregate mixture in the concrete, the sizes of aggregates, etc. need to be properly accounted for. Therefore, the relation between the strength and fracture energy of concrete seems not to be in a monotonic manner. Also note that a steeper slope in the regression line of the test data does not necessarily mean a higher fracture energy for the material.

## 6. Conclusions

The major conclusions of this study can be summarized as follows:

- 1) A certain amount and proper size of coarse aggregate in the HPC is beneficial to the concrete strength and fracture energy. Based on the size-effect law, the hardened high-performance concrete has a much higher fracture energy (68.3 N/m) than the comparable hardened mortar (22.5 N/m), binder paste (3.48 N/m) and cement paste (3.4 N/m).
- 2) In addition to the compressive strength, the packing structure of aggregate mixture and the sizes of aggregate particles, etc. also play a very important role in determining the fracture energy of high-performance concrete. Same volumetric amount of aggregate but with different size gradation used in the high-performance concrete will substantially alter the fracture properties of concrete.
- 3) The correlation between the strength and fracture energy of concrete is

---

not monotonic nor unique. There seems exist an optimal fracture energy for all kinds of the high-performance concrete.

## 7. Acknowledgments

The financial support of NSC86-2211-E-011-004 to this study from the National Science Council, Taiwan, R.O.C. is highly appreciated.

## 8. References

- Aitcin, P.-C. and A. Neville (1993) High-Performance Concrete Demystified, **Concrete International**, Vol. 15, No. 1, Jan. 1993, 21-26.
- Bazant, Z. P. and Pfeiffer, P. A. (1987) Determination of Fracture Energy from Size Effect and Brittleness Number, **ACI Materials Journal**, Vol. 84, No.6, 463-480.
- Gettu, R., Bazant, Z.P., and Martha, E.K.(1990) Fracture Properties and Brittleness of High-Strength Concrete, **ACI Materials Journal**, Nov-Dec., pp. 608-618.
- Gutiérrez, P. A. and Cánovas, M. F. (1996) High-Performance Concrete: Requirements for Constituent Materials and Mix Proportioning, **ACI Materials Journal**, Vol. 93, No. 3, 233-241.
- Hillerborg, A., Modeer, M., Petersson, P.-E. (1976) Analysis of Crack Formation and Crack Growth in Concrete by Means of Fracture Mechanics and Finite Elements, **Cement and Concrete Research**, Vol. 6, No. 6, 773-782.
- Jenq, Y. S. and Shah, S. P. (1985) A Two Parameter Fracture Model for Concrete, **Journal of Engineering Mechanics, ASCE**, Vol. 111, No. 4, 1227-1241.
- Mehta, P.K. and P.-C. Aitcin (1990) Principles Underlying Production of High-Performance Concrete, **Cement, Concrete and Aggregate**, Vol. 12, No.. 2, Winter, 70-78.
- Okamura, H, (1997) Self-compacting High-Performance Concrete, **Concrete International**, July, 50-54.
- Perdikaris, P. C. and Romeo, A. (1995) Size Effect on Fracture Energy of concrete and Stability Issues in Three-Point Bending Fracture Toughness Testing, **ACI Materials Journal**, Vol. 92, No. 5, 483-496.

## THE INFLUENCE OF THE TYPE OF COARSE AGGREGATES ON THE FRACTURE MECHANICAL PROPERTIES OF HIGH- STRENGTH CONCRETE

M. Hassanzadeh,  
Swedish National Testing and Research Institute  
Department of Building Technology  
Borås, Sweden

### Abstract

The paper investigates the effects of geologically different types of crushed coarse aggregate on the strength, stiffness and fracture energy of high-strength concrete. The results show that the strength, stiffness and fracture energy of concrete depend on the type of aggregate. However, the results do not reveal the existence of any significant correlations between the mechanical properties of the rocks, which the aggregates are made of, and the fracture energy and compressive strength of concrete.

Key words: coarse aggregates, fracture energy, High-strength concrete

### 1 Introduction

In a normal-strength concrete, by which is meant concrete with water/binder ratio greater than 0.4, the strength of the aggregate is normally higher than the mortar and the interfacial transition zone. Hence, in a

normal-strength concrete the fracture processes mainly take place within the mortar, by which is meant hydrated and unhydrated binder and pores, and the interfacial transition zone. In a high-strength concrete, however, due to the low water/binder ratio and perhaps addition of the silica fume, the strength of the mortar and the interfacial zone can be sufficiently high to involve the aggregates in the fracture processes. Since the strength of the mortar and the interfacial transition zone increase with decreasing water/binder ratio the involvement of the aggregates in the fracture processes increases with decreasing water/binder ratio, Tasdemir et al. (1995).

The volume fractions of the mortar, the fine aggregates and the coarse aggregates in concrete are approximately 30%, 35% and 35% respectively, i.e. the volume fraction of the coarse aggregates is approximately the same as that of the mortar. Since, in a high-strength concrete the coarse aggregates are involved in the fracture processes as well as the surrounding mortar the fracture behaviour of aggregates and their influences on the fracture mechanical properties of concrete should not be neglected when designing high-strength concrete.

This paper presents results of tests which were conducted in order to investigate the effects of the geologically different crushed coarse aggregates, particle size between 8 and 16 mm, on the strength, stiffness and fracture energy of the high-strength concrete.

## 2 Method

### 2.1 Concrete compositions

The concrete mixes which were used in the investigation differ with regard to the water/binder ratio, W/B ratio, the content of the silica fume and the type of the coarse aggregates. The binders and the water/binder ratios which were used are shown in Table 1.

Table 1. The binders and the water/binder ratios

Binder	Water/binder ratio		
Ordinary portland cement, (OPC)	0.30	0.40	0.55
OPC and silica fume (S), (OPCS) S/OPC = 0.05	0.30	0.40	

The coarse aggregates are defined as the crushed particles with a particle size between 8 and 16 mm. The aggregates were diabase (DB), fine-grained granite (GF), medium-grained granite (GM), gneiss (GN),

quartzite (QS) and quartzite (QH). The aggregates were from different locations in Sweden. The fine aggregates, which are defined as natural particles with a particle size between 0 - 8 mm, were the same for all the concrete mixes. The ratio between the coarse and the fine aggregates was 1.5 in all concrete mixes. The volume fraction of the aggregates was 0.67 in all concrete mixes.

The total number of concrete mixes was 30, i.e. 5 (mortars) x 6 (coarse aggregate types).

## 2.2 Tests

The compressive,  $f_{cc}$ , the tensile splitting,  $f_{ct}$ , the flexural,  $f_{cf}$ , and the net flexural,  $f_{cf,net}$ , strengths of concrete were determined. Furthermore, the compressive modulus of elasticity,  $E_{cc}$ , and the fracture energy,  $G_F$ , of the concrete were determined. The compressive strength was determined by means of cubic specimens, 100 mm edge size. The splitting tensile strength was determined by means of cylindrical specimens, 200 mm length and 100 mm diameter. The compressive modulus of elasticity, i.e. unloading secant modulus within the stress limits 0.5 MPa -  $f_{cc,cyl}/3$ , was determined by means of cylindrical specimens. The fracture energy was determined by means of three-point bend tests according to the RILEM TC50 draft recommendation. The beam length, width and depth were 840 mm, 100 mm and 100 mm respectively. The net flexural strength was determined by means of the fracture load of the specimens which were used in the fracture energy tests. The flexural strength was determined by means of three-point bend tests on the halves of the beams which were used in the fracture energy tests.

All specimens were cast in steel moulds from the same batch. The specimens were demoulded the day after casting and were stored in the lime saturated water until the day of testing at 28 days of age. However, in accordance with Swedish standards, the compressive test specimens were removed from the water five days after casting. The specimens were stored in the laboratory climate until the day of testing at 28 days of age.

The mechanical properties of the aggregates were also determined. The tests were performed on the cores which were drilled at the production sites of the aggregates. The core diameter was 60 mm. The properties which were determined are compressive and the tensile splitting strength, the modulus of elasticity and the fracture energy. The length of the specimens was 120 mm in the first three tests and 300 mm in the fracture energy tests. In the fracture energy tests the depth of the notch was half of the core diameter.

### 3 Test results

The mechanical properties of the concrete mixes and the rocks, coarse aggregates, are shown in Table 2 and Figure 1 respectively. The results corresponds to the mean values of at least three tests.

Table 2. Test results

W/B ratio	Agg.	$f_{cc}$ MPa	$f_{ct}$ MPa	$f_{cf}$ MPa	$f_{cfnet}$ MPa	$E_{cc}$ GPa	$G_F$ N/m
0.30 OPC	DB	129	6.4	10.3	8.4	51	191
	GN	120	6.3	9.0	7.2	39	146
	GF	114	6.3	9.0	6.7	42	163
	GM	121	5.9	8.0	7.3	41	164
	QS	126	6.9	9.5	7.7	41	170
	QH	124	5.9			41	147
0.40 OPC	DB	84	5.2	8.0	6.3	44	199
	GN	86	4.6	6.1	6.1	34	144
	GF	82	5.2	7.7	5.9	37	163
	GM	93	4.9	7.6	6.1	36	170
	QS	93	5.2	7.2	6.1	36	201
	QH	90	5.0			36	129
0.55 OPC	DB	55	4.3	5.4	5.2	38	133
	GN	55	4.3	7.0	5.1	29	128
	GF	58	4.4	6.3	6.0	33	193
	GM	57	4.0	7.0	5.1	32	130
	QS	57	4.8	6.4	5.3	31	152
	QH	56	3.7			32	128
0.30 OPCS	DB	126	6.3	10.5	7.8	49	161
	GN	131	6.2	10.6	7.5	40	139
	GF	121	6.8	10.8	8.8	42	192
	GM	129	6.3	10.8	7.9	42	174
	QS	135	7.1	10.2	8.3	42	160
	QH	128	6.5			42	176
0.40 OPCS	DB	104	5.8	7.8	6.6	45	161
	GN	104	5.0	7.2	6.4	33	154
	GF	102	5.5	7.9	6.8	38	144
	GM	96	5.2	7.9	6.3	37	145
	QS	104	5.9	8.1	6.9	35	154
	QH	101	5.7			38	163

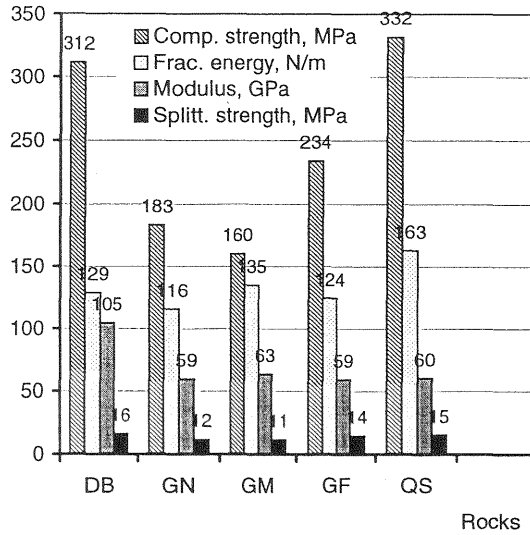


Fig. 1. Mechanical properties of coarse aggregates

## 4 Discussion

### 4.1 Compressive and splitting strength

Figure 2 shows the compressive strength of the concretes as functions of the W/B ratio. The curves are obtained by fitting equation 1 to the results of the compressive tests. As the figure shows, the effect of the type of coarse aggregate on the compressive strength is not considerable. The reason may be that the aggregates which were used had, in comparison with concrete, relatively high strength. Furthermore, application of statistical methods has not revealed any significant correlations between any of the fracture mechanical properties of the aggregates and the compressive strength of the concrete.

$$f_{cc} = K \cdot \left( \frac{1}{wbr_{eff}} - a \right) \quad (1)$$

$$wbr_{eff} = \frac{W}{C + \beta \cdot S}$$

$K$  and  $a$  are curve fitting constants.  $W$ ,  $C$  and  $S$  are the contents of water, cement and silica fume respectively.  $\beta$  is an efficiency factor which was equated to 2 during curve fitting.

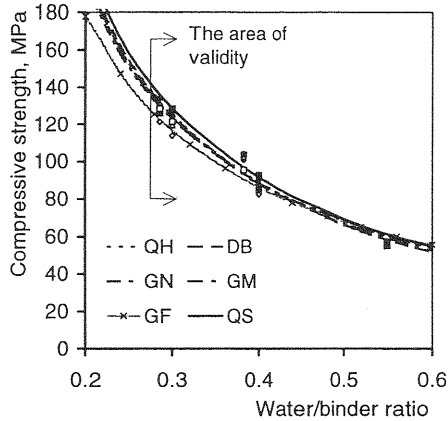


Fig. 2 The compressive strength as a function of W/B ratio

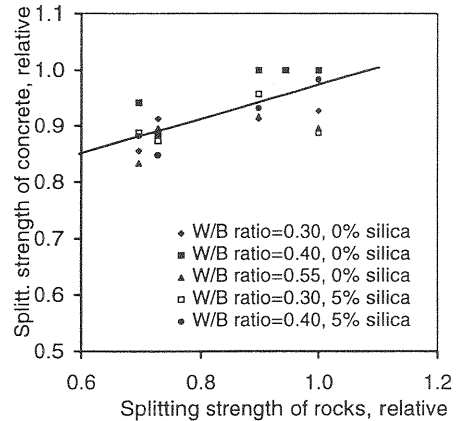


Fig. 3 The relative splitting strength of concrete as a function of the relative splitting strength of rocks

In contrast to the compressive strength the results of the splitting tests show that the splitting strength of concrete is to some extent influenced by the splitting strength of aggregates, Figure 3.

The modulus of elasticity of diabase is 105 GPa which is considerably greater than the modulus of elasticity of the other rocks. As can be observed in Table 2 the modulus of elasticity of concretes which contain diabase is greater than concretes containing the other types of aggregate.

#### 4.2 Fracture energy and characteristic length

Figure 4 shows the variation of fracture energy with the W/B ratio for concretes which contain different types of coarse aggregates. The concretes which are presented in the figure do not contain silica fume. As the figure shows, the fracture energy increases with decreasing W/B ratio in two cases whereas in one case it decreases. Furthermore, in three cases the fracture energy assumes a maximum value in the intermediate range of the W/B ratio. Application of statistical methods has not revealed any significant correlations between any of the fracture mechanical properties of the rocks and the fracture energy of the concrete. The reason may be

that besides the fracture mechanical properties of the aggregates, assuming that the mechanical properties of the aggregates are the same as the rocks, other properties such as the particle form, the mineralogy, and the roughness of the surface of the aggregates may have effects on the fracture energy. Perhaps these properties play an important role when considering the micro-cracking which takes place outside of the fracture process zone. These effects of the mentioned properties on the fracture energy have not been investigated.

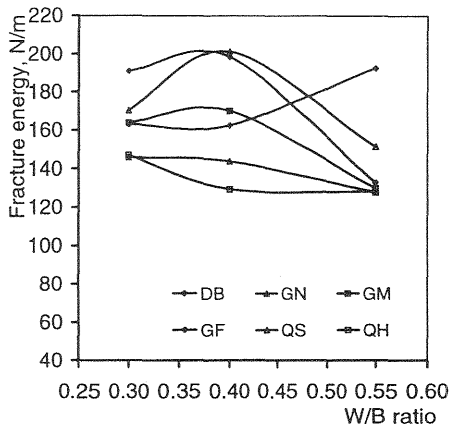


Fig. 4 Influence of the aggregate type and W/B ratio on the fracture energy of concrete, 0% silica content

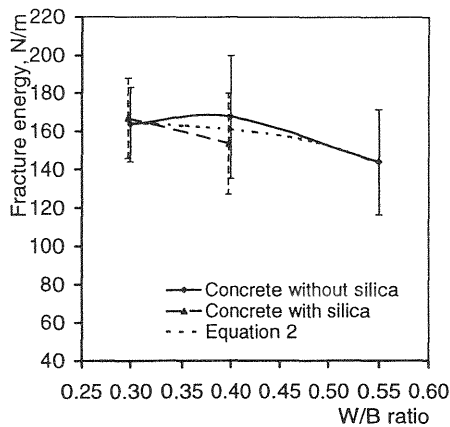


Fig. 5 The influence of W/B ratio on fracture energy of concrete

Disregarding concrete containing gneiss, the fracture energy increases with decreasing W/B ratio when silica fume is included, Table 2. For concretes with 0.4 W/B ratio the addition of the silica fume has a negative effect on the fracture energy except for concrete made of quartzite H. For concretes with 0.3 W/B ratio the addition of the silica fume has a negative effect on the fracture energy in 50% of cases.

Figure 5 shows the variation of the fracture energy with W/B ratio. The data in the figure corresponds to the mean value of all the fracture energy tests irrespective of the type of aggregate. Furthermore, the figure shows a mathematical function, equation 2, fitted to all results irrespective of the content of the silica fume and the type of aggregate.

$$G_f = 166 \cdot (1 - e^{10(W/B - 0.75)}) \quad N / m \quad 0.30 \leq W / B \leq 0.55 \quad (2)$$

In handbooks and design codes the fracture energy is normally expressed as a function of the compressive strength. Figure 6 shows the results of the fracture energy tests as a function of compressive strength. As can be observed, the compressive strength is not an appropriate parameter to express the fracture energy of the concrete. The figure also shows also a mathematical function, equation 3, fitted to the test results. The values  $\pm 15$  are the limits of the 95% confidence intervals of the function. Furthermore, the figure shows the fracture energy as a function of compressive strength according to the CEB-FIP's Model Code 1990. It should be noted that the cylinder compressive strength of CEB has been converted to the cube compressive strength by using the multiplication factors  $1.05 \times 1.35$ .

$$G_F = 168 \cdot (1 - e^{-0.035 f_{cc}}) \pm 15 \quad N / m \quad 50 \leq f_{cc} \leq 140 \text{ MPa} \quad (3)$$

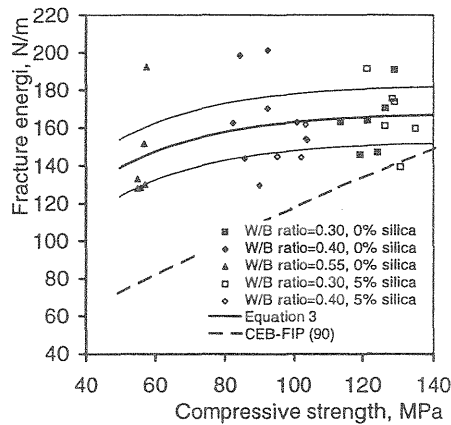


Fig. 6 Fracture energy as a function of compressive strength

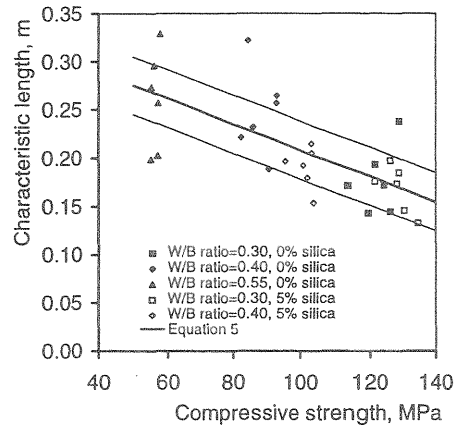


Fig. 7 Characteristic length as a function of compressive strength

The brittleness of concrete can be expressed by its characteristic length  $l_{ch}$  (m), Petersson (1981).

$$l_{ch} = \frac{E \cdot G_F}{f_t} \quad (4)$$

$E$ ,  $G_F$  and  $f_t$  are modulus of elasticity, fracture energy and uniaxial tensile strength respectively. However, in this investigation  $f_t$  has been equated to  $f_{ct}$ .

As far as the effects of the W/B ratio and the types of the aggregates on the characteristic length are concerned, the same tendencies as the fracture energy are observed. Furthermore, the results show that the brittleness of concrete increases with increasing strength, Figure 7. The figure also shows a mathematical function, equation 5, fitted to the test results.

$$l_{ch} = (-134 \cdot 10^{-3} \cdot f_{cc} + 0.34) \pm 0.03 \quad m \quad 50 \leq f_{cc} \leq 140 \text{ MPa} \quad (5)$$

### 4.3 Flexural and net flexural strength

Both flexural and net flexural strength increase with decreasing W/B ratio. The influence of the coarse aggregates on these parameters is the same as in the case of the splitting tensile strength. Figure 8 shows the flexural and the net flexural strength as functions of the compressive strength. As can be observed the difference between the flexural and net flexural strength increases with increasing strength. The results indicate that the crack sensitivity of the concrete increases with increasing strength.

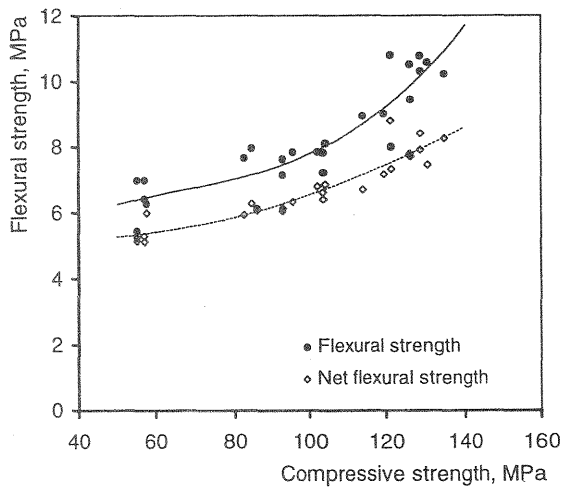


Fig. 8 The flexural and the net flexural strength as functions of the compressive strength

---

## 5 Conclusions

The types of coarse aggregate used in this investigation have little effect on the compressive strength of concrete. Furthermore no significant correlations between any of the fracture mechanical properties of the aggregates and the compressive strength of concrete have been observed.

The results show that both splitting tensile strength and modulus of elasticity of the concrete are influenced by the splitting tensile and modulus of elasticity of the aggregates.

The tests show that the type of aggregate has a considerable effect on the fracture energy when it is expressed as a function of the W/B ratio. Depending on the type of the aggregate the fracture energy may increase, or decrease by decreasing W/B ratio, or assume a maximum value in the intermediate range of the W/B ratio.

According to the results the brittleness and the crack sensitivity of the concrete increase with increasing strength of the concrete.

## Acknowledgements

This investigation was a part of the Swedish national project dealing with high-performance concrete. This investigation has been conducted with the aid of financial support from Cementsa, Elkem, Euroc Beton, NCC Bygg, SKANSKA, Strängbetong, The Swedish Council for Building Research (BFR) and Swedish National Board for Industrial and Technical Development (NUTEK). The project was conducted at the Division of Building Materials, Lund Institute of Technology, Sweden.

## References

- Petersson, P.E. (1981) **Crack growth and development of fracture zone in plain concrete and similar materials**, Report TVBM-1006, Div. of Building Materials, Lund Institute, Lund, Sweden.
- Tasdemir, C., Tasdemir, M.A., Grimm, R. And König, G. (1995) Micro-structural effects on the brittleness of high strength concrete, in **Fracture Mechanics of Concrete Structures** (ed. F.H. Wittmann), AEDIFICATIO Publishers, Germany, 125-134.

## INFLUENCE OF AGGREGATE SHAPE ON THE FRACTURE BEHAVIOUR OF CONCRETE

K. M. El-Sayed, G. V. Guinea, C. Rocco, J. Planas , and M. Elices,  
Departamento de Ciencia de Materiales, E.T.S.I. Caminos,  
Universidad Politécnica de Madrid  
Spain

### Abstract

Coarse aggregate has a prominent role in the mechanical behaviour of concrete. The shape and size of aggregate particles are known to affect the fracture properties. This paper reports a preliminary experimental research into this influence using the cohesive crack model as a framework. Concrete batches with rounded and crushed aggregates of different sizes and grading are considered. The mechanical behaviour is determined with conventional standard tests (compression and splitting) as well as with fracture tests such as the three-point bending beam. The results show a marked influence of the shape of aggregates on the fracture properties and on the tail of the softening curve.

Key words: aggregates, concrete, fracture, softening, internal structure.

### 1 Introduction

Plain concrete is a heterogeneous material formed by the combination of a hardened cement paste and particles of rock. From a mechanical point of view it is helpful to consider concrete as a two phase material with a matrix made of cement and fine aggregates (mortar), and a particulated reinforcement (coarse aggregates). This approach is useful when analyzing the influence of the aggregates on the mechanical performance of concrete, particularly on the fracture behaviour, which is known to be affected by the size, shape and grading of the coarser aggregates.

In order to quantify the macroscopic fracture properties of concrete a cohesive crack model is assumed. This has been a successful approach since its proposal by Hillerborg and co-workers (1976).

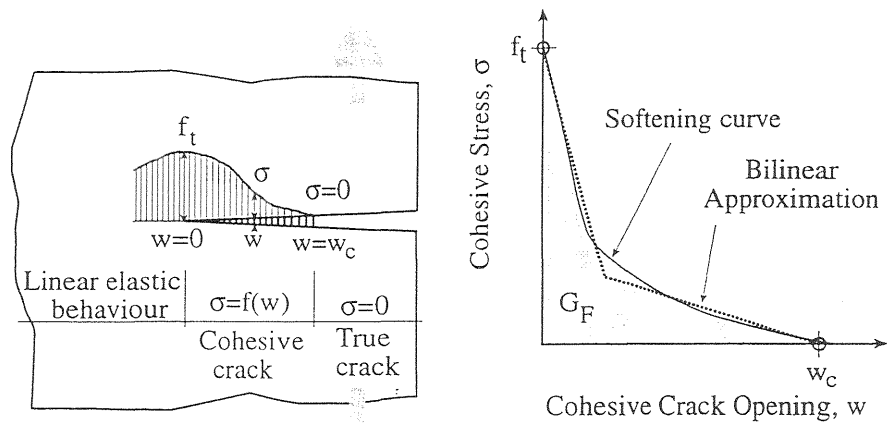


Fig. 1 Cohesive crack in mode I loading and softening function.

In this model the material response is completely determined by the softening curve, a material function that univocally relates the stress transferred through the crack faces -the cohesive stress- and the crack opening at a given point.

For a crack under mode I loading (Fig.1), which is the most common testing situation, the cohesive stress is normal to the crack plane, and progressively decreases from  $f_t$ , the tensile strength, at the tip of the cohesive crack, to zero at the point where the opening reaches  $w_c$ , the critical crack opening.

The area under the softening curve is the work supply needed to fully open a unit surface of crack, and so called the *specific fracture energy*,  $G_F$  (or simply, fracture energy). The fracture energy,  $G_F$ , the tensile strength,  $f_t$ , the critical crack opening,  $w_c$ , as the softening function itself, are all of them macroscopic material properties, and thus dependent on the internal structure of concrete.

To simplify, the softening function is often approximated by a bilinear function. This simple diagram suffices to suitably describe the pre-peak as well as the post-peak behaviour of the material (Petersson 1981, Guinea, Planas and Elices 1994).

In recent years many experimental studies have been carried out to ascertain the influence of aggregates on the fracture parameters of concrete, mainly concentrating on the effects of the maximum aggregate size and on the quality of the aggregate.

The type of aggregate plays a paramount role in the fracture mechanisms and in the fracture response of concrete. Depending on the strength of the aggregate and of its interface with the matrix, the crack propagation goes through the particles or around them, thus resulting in a

different crack roughness. This influences the energy consumption and the interlock effects, and has a direct effect on concrete toughness (Pettersson 1981, Cornelissen and Hordijk 1986, and Elices, Guinea and Planas 1992a). A good selection of the aggregate is a solid basis to make a good concrete. However, for economic reasons, the kind of aggregate is usually restricted to the material available locally, and shape and grading are the only possible choices.

The dependence of fracture behaviour on the maximum aggregate size,  $d_{max}$ , has been observed by many authors, although the large scatter usually present in the results make it difficult to arrive at definite conclusions. Based on the results of a comparative study organized by RILEM-TC50, Hillerborg (1985) concluded that there is a tendency to increase the fracture energy as the maximum aggregate size becomes larger. The same trend was reported by Mihashi (1992) who also analyzed the effect of  $d_{max}$  on the softening curve.

In this paper some preliminary results are presented to show the influence of the size, shape and grading of aggregates on the fracture parameters of concrete, using the cohesive crack model as a framework. Section 2 describes the concrete mixes and the tests carried out to characterize them, and in Section 3 the results are discussed.

## 2 Experimental program

### 2.1 Materials

Ordinary Portland cement (ASTM Type I) and siliceous aggregates –all from the same natural deposit– were used throughout the testing program. Silica sand with a fineness modulus of 2.5 and maximum size of 4 mm, and rounded and crushed granite with sizes up to 20 mm, were used as fine and coarse aggregate, respectively. To preserve the parent rock, crushed particles were obtained by grinding oversized fractions of rounded aggregates.

Ten batches were cast, as summarized in Table 1. The cement content was 400 kg/m<sup>3</sup> and the ratios water/cement, sand/cement and coarse aggregate/cement were 0.48, 1.78 and 2.63, respectively. The volume fraction of coarse aggregate was kept constant and equal to 40% in all the batches.

From one batch to another only the coarse aggregate was changed. Two shapes, rounded and crushed, three maximum sizes of 10, 12.5 and 20 mm and two gradings, continuous and uniform, were tested.

Crushed and rounded aggregates were classified in three different size fractions: 5-10 mm, 10-12.5 mm and 12.5-20 mm. The uniform grading was formed with only one of these fractions. The continuous grading met the requirements of ASTM C33, and was obtained by combining two or three different fractions.

Table 1 Composition of the concrete batches

Batch	$d_{max}$ (mm)	Grading	Aggregate Shape
RU-10	10.0	Uniform	Rounded
RU-12	12.5	Uniform	Rounded
RU-20	20.0	Uniform	Rounded
RC-12	12.5	Continuous	Rounded
RC-20	20.0	Continuous	Rounded
BU-10	10.0	Uniform	Crushed
BU-12	12.5	Uniform	Crushed
BU-20	20.0	Uniform	Crushed
BC-12	12.5	Continuous	Crushed
BC-20	20.0	Continuous	Crushed

## 2.2 Mechanical Characterization

Three groups of experiments were carried out to determine the mechanical behaviour for each concrete batch : standard compression test, splitting tests and stable three point bend fracture tests.

Compression tests were performed according to ASTM C39 and ASTM C469 standards to measure the compressive strength,  $f_c$ , and the modulus of elasticity in compression,  $E_c$ . The test specimens were cylinders 150 mm in diameter and 300 mm in height.

Stable splitting tests to measure the tensile strength,  $f_t$ , were conducted on cylinders with the same dimensions as in the compression tests, following a procedure described elsewhere (Rocco, 1996).

Three point bend tests on half-notched beams were performed according the RILEM method (RILEM, 1985), enhanced with some additional suggestions by the authors (Guinea, Planas and Elices, 1992; Planas, Elices and Guinea, 1992; Elices, Guinea and Planas, 1992b). Beams of 100 x 100 x 430 mm<sup>3</sup> with a central notch 2 mm wide and 50 mm deep were tested on bending, with span to depth ratio equal to 4. From these tests the fracture energy,  $G_F$ , the critical crack opening,  $w_c$ , and the shape of the bilinear softening curve were determined.

From each concrete batch a complete set of specimens were cast, each composed of 5 beams for fracture tests and 8 cylinders; 4 for the compression tests and 4 for the splitting tests.

## 3 Results and Discussion

The results for the 10 concrete batches are summarized in Table 2. Fracture parameters were determined following the bilinear fit procedure by the authors (Guinea, Planas and Elices, 1994).

Fig. 2 plots the compressive strength vs. the maximum aggregate size. The use of crushed aggregates give higher strengths than rounded, with  $f_c$  values close to those of the mortar matrix. This effect has been widely

reported in the literature and seems to be dependent on the mechanical bond between matrix and aggregates, which is highly influenced by the shape of aggregates (Neville, 1981). The compressive strength has a maximum when varying the aggregate size, and decreases when large aggregates are incorporated, as a consequence of lowering the bond area. This could also explain the effect of the grading, where a continuous distribution gives a concrete with better resistance to compression.

In the case of the elastic modulus the aggregate has a second order effect. All the values for concrete batches in Table 2 are within a 10% variation, close to the magnitude of estimated error.

Table 2 Characterization tests. Mean values and 68% confidence interval.

Batch	$f_c$ (MPa)	$E_c$ (GPa)	$G_F$ (N/m)	$f_t$ (MPa)	$w_c$ ( $\mu$ m)
Mortar	49.5 $\pm$ 0.7	28.4 $\pm$ 0.4	58 $\pm$ 2	3.55 $\pm$ 0.08	174 $\pm$ 8
RU-10	45.9 $\pm$ 1.0	38.4 $\pm$ 0.2	74 $\pm$ 4	3.11 $\pm$ 0.05	197 $\pm$ 5
RU-12	46.6 $\pm$ 0.6	38.7 $\pm$ 0.3	91 $\pm$ 8	3.15 $\pm$ 0.06	240 $\pm$ 18
RU-20	43.5 $\pm$ 0.5	39.8 $\pm$ 0.3	84 $\pm$ 15	2.62 $\pm$ 0.05	294 $\pm$ 83
RC-12	47.4 $\pm$ 0.7	38.6 $\pm$ 0.5	93 $\pm$ 5	3.11 $\pm$ 0.09	231 $\pm$ 7
RC-20	44.3 $\pm$ 0.6	36.6 $\pm$ 2.0	74 $\pm$ 4	2.91 $\pm$ 0.03	262 $\pm$ 29
BU-10	48.8 $\pm$ 0.7	38.3 $\pm$ 0.3	100 $\pm$ 9	3.48 $\pm$ 0.07	198 $\pm$ 9
BU-12	52.4 $\pm$ 0.9	38.8 $\pm$ 0.2	116 $\pm$ 6	3.46 $\pm$ 0.05	219 $\pm$ 7
BU-20	46.6 $\pm$ 0.9	39.6 $\pm$ 0.1	141 $\pm$ 6	2.98 $\pm$ 0.08	234 $\pm$ 13
BC-12	53.5 $\pm$ 0.5	38.9 $\pm$ 0.4	106 $\pm$ 6	3.59 $\pm$ 0.07	210 $\pm$ 14
BC-20	48.9 $\pm$ 0.7	38.6 $\pm$ 0.4	119 $\pm$ 8	3.23 $\pm$ 0.09	229 $\pm$ 10

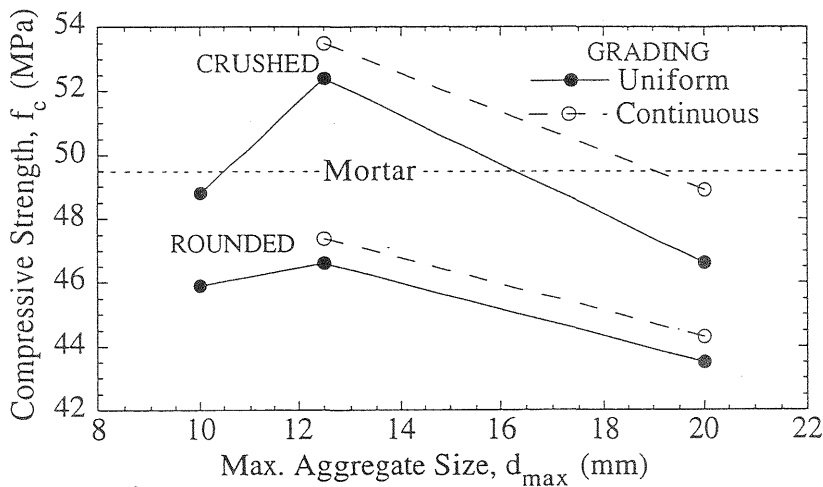


Fig. 2. Influence of aggregates on the compressive strength

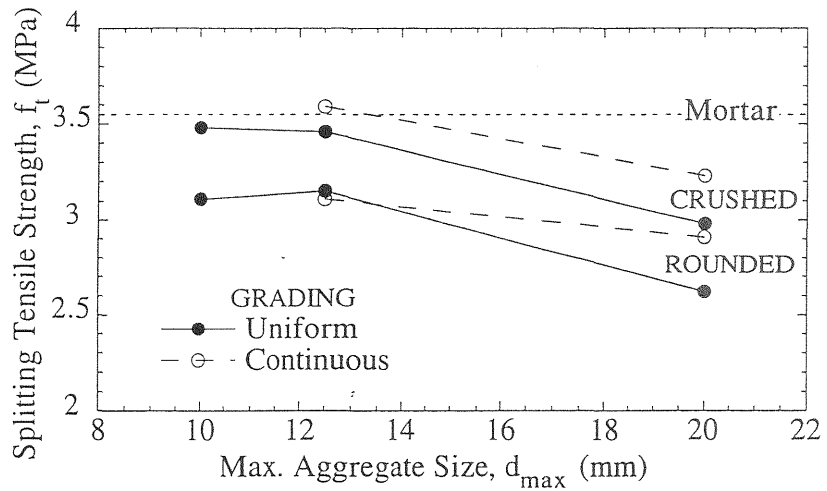


Fig. 3. Influence of aggregates on the tensile strength

The tensile strength has a behaviour similar to the compressive strength (Fig. 3). Again, the use of a rougher aggregate (crushed) gives concretes with higher resistance, and this resistance decreases as the aggregate size becomes larger. As with the compressive strength, there is a small increment of resistance when a continuous grading is introduced in the mix.

The origin of these effects is probably the reduction in bond area produced when increasing the maximum aggregate size –or when using a uniform grading– while keeping constant the volume of aggregate.

With regard to fracture properties, the influence of the shape, size and grading of aggregates seems to be important. Fig. 4 shows the results for the fracture energy, whose values undergo a significant increment when crushed aggregates are used instead of rounded ones.

This behaviour can be due to the greater energy consumption to break the aggregates compared to the debonding mechanism. Thus, a larger fracture energy is obtained when the fraction of broken particles is dominant, which is the case of the batches made with crushed aggregates. This has been quantified for concretes with uniform grading where the ratio of broken surface to debonded surface of aggregates is close to 16% when using rounded particles, whereas it increases to 37% for concretes with crushed aggregates.

This phenomenon is congruent with the large values of  $w_c$  measured in concretes with rounded aggregates, as shown in Fig. 5. In this case, the presence of debonded particles forces the crack path to be more rough, intensifying the interlock mechanism and thus transferring stresses at wider crack openings.

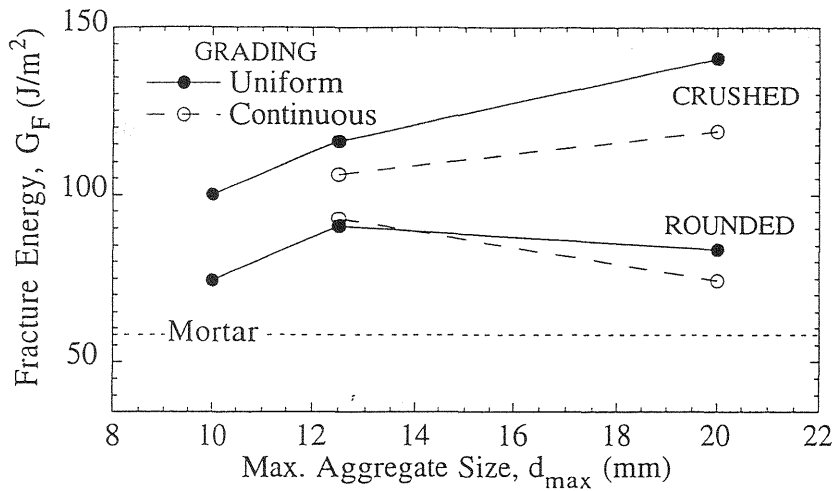


Fig. 4. Influence of aggregates on the fracture energy

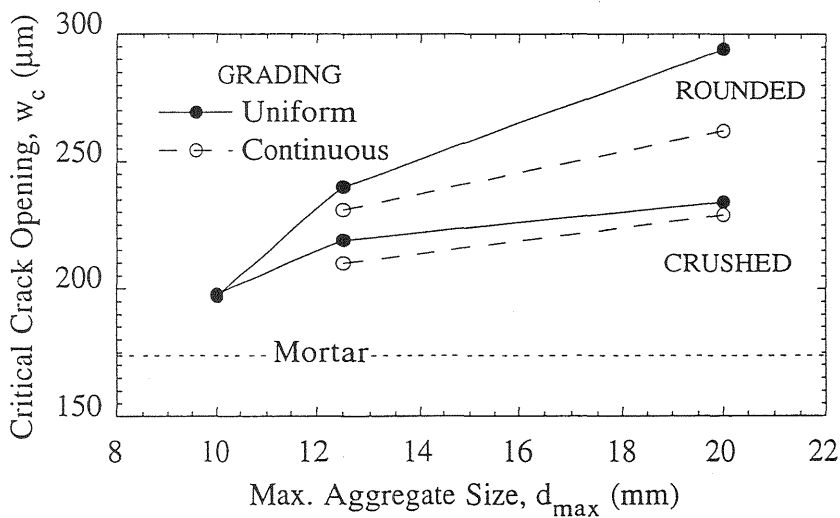


Fig. 5. Influence of aggregates on the critical crack opening

The effect of the maximum aggregate size on the fracture energy is dependent on the shape of the aggregate. Concrete batches with crushed aggregates show a moderate increment of  $G_F$  as  $d_{max}$  increases, whereas the use of rounded particles makes  $G_F$  nearly insensitive to aggregate size within the range analyzed (Fig.4). Uniform and continuous grading present the same behaviour but always giving the continuous distribution the lower values of  $G_F$ . The same applies to  $w_c$  (Fig.5)..

Regarding the shape of the softening curve, Figs. 6 and 7 plot the non-dimensional representation of the softening functions measured for the concretes with uniform grading. Fig. 6 shows that concrete with rounded aggregates give a similar softening, close to the behaviour of the mortar matrix. When the aggregate is crushed, the softening function seems to depend on the maximum size, reducing the tail as the particles become larger while keeping nearly the same initial descending part.

A comparison between the two sets of softenings of Figs. 6 and 7 shows that concretes with rounded aggregates have a longer tail, due probably to the interlocking mechanism mentioned before.

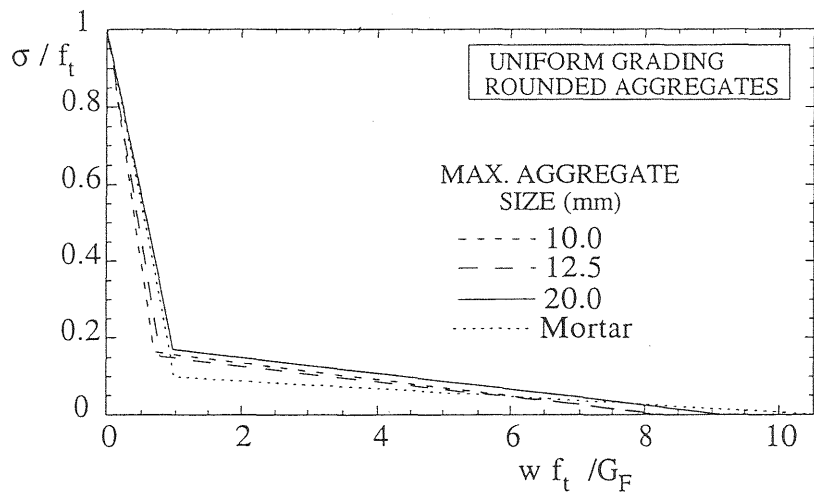


Fig. 6. Influence of rounded aggregates on the softening curve

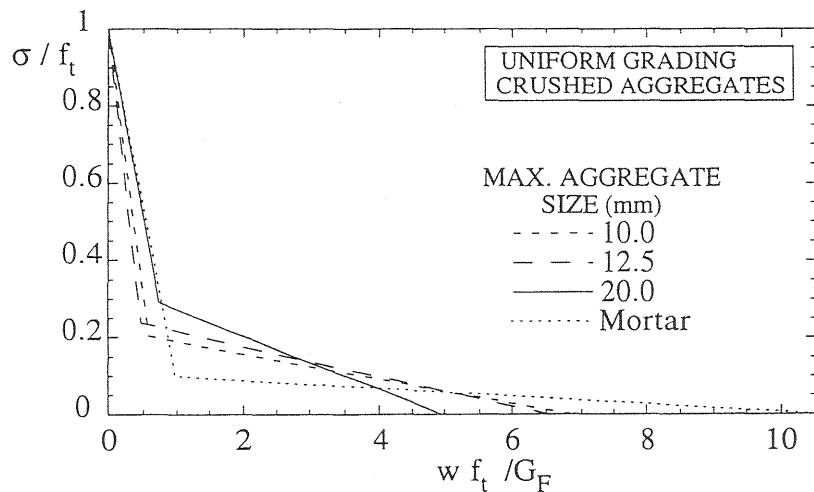


Fig. 7. Influence of crushed aggregates on the softening curve

#### 4 Acknowledgments

The authors gratefully acknowledge financial support for this research provided by the Comisión Interministerial de Ciencia y Tecnología, Spain, under grants MAT94-0120-C03 and MAT97-1022 and by the Ministerio de Educación y Ciencia through the Foreign Scientists Program. The authors also thanks the company Portland-Valderribas for supplying the cement used in this research.

#### 5 References

- CEB-FIP Model Code 1990-Final Draft (1991), **Comite Euro-International du Beton**, Bulletin d'Information, 203.
- Cornelissen, H.A.W., Hordijk, D.A. and Reinhardt, H.W. (1986) Experiments and Theory for the application of fracture mechanics to normal and lightweight concrete, in **Fracture Toughness and Fracture Energy of Concrete**, (ed. F.H.Wittmann, Elsevier Science Publishers B.V), Amsterdam, 565-575.
- Elices, M., Guinea, G.V. and Planas, J. (1992a) Choosing the right concrete for piles: an application in concrete fracture mechanics, in **Fracture Mechanics of Concrete Structure**, (ed. Zdenek P. Bazant, Elsevier Science publishers LTD), Colorado, USA, 782-787.
- Elices, M., Guinea, G.V. and Planas, J. (1992b) Measurement of the fracture energy using three point bend tests: Part 3– Influence of cutting the P- $\delta$  tail, **Mat. and Struct.**, 25, 327-334.
- Guinea, G.V., Planas, J. and Elices, M. (1992) Measurement of the fracture energy using three point bend tests : Part 1– Influence of experimental procedures, **Mat. and Struct.**, 25, 212-218.
- Guinea, G.V., Planas, J. and Elices, M. (1994) A general bilinear fit for the softening curve of concrete. **Materials and Structures**, 27, 99-105.
- Hillerborg, A. (1985) Results of three comparative test series for determining the fracture energy  $G_F$  of concrete. **Materials and Structures**, 18, 407-413.

- 
- Hillerborg, A.M, Modeer, M., and Petersson, P.E. (1976) Analysis of crack formation and crack growth in concrete by means of fracture mechanics and finite elements. **Cement and Concrete Research**, 6, 773-782.
- Mihashi, H. (1992) Material structure and tension softening properties of concrete, in **Fracture Mechanics of Concrete Structures**, (ed. Zdenek P. Bazant, Elsevier Science Publishers LTD), Colorado, USA, 239-250.
- Neville, A.M. (1981) **Properties of Concrete**, Pitman, London
- Petersson, P.E. (1981) Crack growth and development of fracture process zone in plain concrete and similar materials, **Report TVBM-1006**, Division of Building Materials, Lund Institute of Technology, Lund, Sweden.
- Planas, J., Elices, M. and Guinea, G.V.(1992) Measurement of the fracture energy using three point bend tests : Part 2– Influence of bulk energy dissipation, **Mat. and Struct.**, 25, 305-312.
- RILEM TC-50 FMC (1985) Determination of the fracture energy of mortar and concrete by means of three point bend tests on notched beams, **Mat. and Struct.**, 18, 285-290.
- Rocco, C. (1996) Size effect and failure mechanisms in the brazilian splitting test ( in Spanish), Ph. D. Thesis, Universidad Politécnica de Madrid.